ACS APPLIED MATERIALS & INTERFACES

Research Article

www.acsami.org

Transport Properties of Amine/Carbon Dioxide Reactive Mixtures and Implications to Carbon Capture Technologies

Salomon Turgman-Cohen,[†,§] Emmanuel P. Giannelis,[‡] and Fernando A. Escobedo*[,†]

[†]School of Chemical and Biomolecular Engineering, Cornell University, Ithaca New York 14853, United States

[‡]Department of Materials Science & Engineering, Cornell University, Ithaca New York 14853, United States

Supporting Information

ABSTRACT: The structure and transport properties of physisorbed and chemisorbed CO_2 in model polyamine liquids (hexamethylenediamine and diethylenetriamine) are studied via molecular dynamics simulations. Such systems are relevant to CO_2 absorption processes where nonaqueous amines are used as absorbents (e.g., when impregnated or grafted onto mesoporous media or misted in the gas phase). It is shown that accounting for the ionic speciation resulting from CO_2 chemisorption enabled us to capture the qualitative changes in extent of absorption and fluidity with time that are observed in thermogravimetric experiments. Simulations reveal that high enough concentration of reacted CO_2 leads to strong intermolecular ionic interactions and the arrest of molecular translations. The transport properties obtained from the simulations of the ionic speciated mixtures are also used to construct an approximate continuum-level model for the CO_2 absorption process that mimics thermogravimetric experiments.

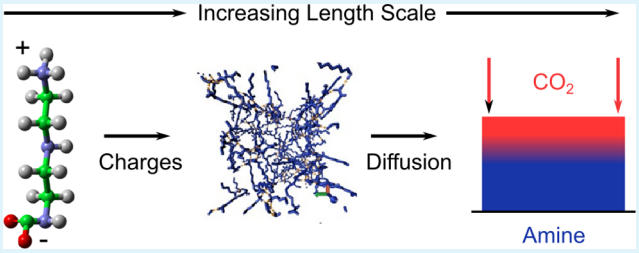

KEYWORDS: *carbon dioxide, sequestration, capture, multiscale, molecular dynamics, polyamines*

INTRODUCTION

Anthropogenic carbon dioxide production has been identified as a cause for global climate warming. Of the total human output of CO_2 to the environment, 52% is produced from single point sources such as power plants and factories.[1] Given the ubiquitous nature of fossil fuels and the paced development of environmentally benign energy technologies, CO_2 capture at single point source producers is a desirable goal to smooth the transition from a fossil fuel economy to that of cleaner and renewable fuel sources.

Amine scrubbing, invented in the 1930s, is the leading technology for CO_2 capture.[2] Current needs to remove CO_2 from flue gases have motivated new developmental efforts in the amine scrubbing process making it a well understood, established technological platform. Unfortunately, amine scrubbing technology has significant disadvantages including the corrosive nature of the aqueous sorbent, the thermal and oxidative degradation of the amine, the energy required to regenerate it, the environmental impact of solvent loses to the atmosphere, and the added costs to produce energy from fossil fuels.[3] Beside amine scrubbing, oxyfuel combustion and calcium looping processes are potential alternatives for industrial deployment.[3]

The typical reaction between amine groups and dry CO_2 involves the formation of ammonium and carbamate ions[4,5]

$$2NH_x + CO_2 \leftrightarrow NH_{x+1}^{+} + NH_{x-1}COO^{-}$$

where x = 1 or 2 for secondary or primary amines, respectively. The sorbent most widely used in the amine scrubbing process is an aqueous solution of monoethanolamine. Aqueous solutions are used because salt formation gives rise to severe kinetic barriers if the sorbent is the pure amine. In fact, it is known that some carbamate/ammonium complexes are stable at room temperature and are capable gelators of several liquids.[6,7] Several suggested approaches to circumvent these kinetic barriers exist, including (i) the use of organic/inorganic composite mesoporous materials[8−16] and (ii) CO_2 capture by a mist of phase changing diamines.[17] Both of these approaches take advantage of the large surface area of amine per volume of the sorbent to limit the effects of kinetic barriers upon CO_2 absorption.

In organic/inorganic hybrid sorbents, thin films of amines are physically or chemically adsorbed to a mesoporous support. In contrast, in the amine spray tower unit operation, small droplets of the amine are created. In both cases, efficient exposure of the CO_2 gas to the amine active component is achieved. The rational development of these alternative technologies requires knowledge of the transport properties of the amine/CO_2 reactive mixtures as a function of CO_2 loading. Of particular interest are the diffusion coefficients of the CO_2 species and the viscosity of the reactive mixture. Also of interest in the case of phase changing sorbents is whether a transition from liquid to solid/gel state occurs. In this work, we focus on the properties of the active amine component in these

Received: October 11, 2014
Accepted: July 22, 2015
Published: July 22, 2015

DOI: 10.1021/acsami.5b04153
ACS Appl. Mater. Interfaces 2015, 7, 17603−17613

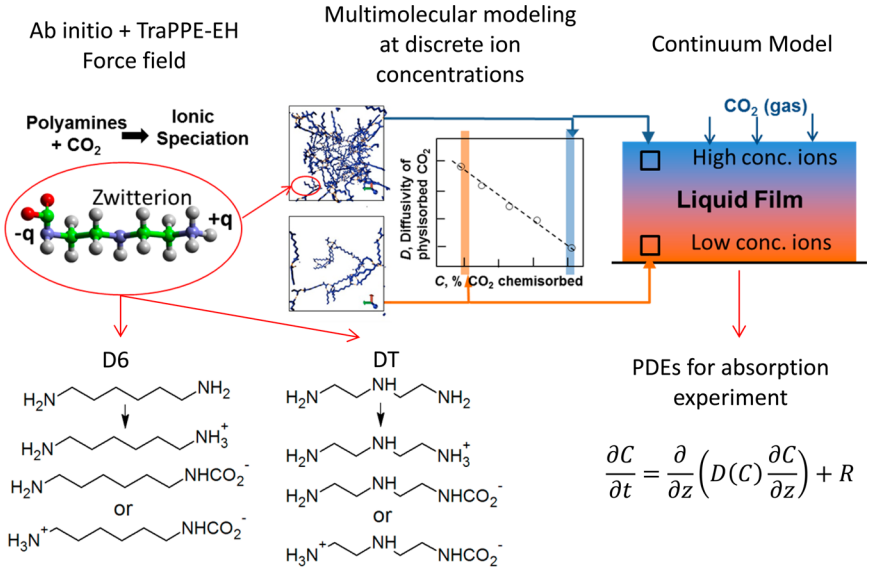

Figure 1. Multiscale procedure followed by this study. Panels from left to right: Ab initio, molecular, and continuum modeling. Molecular modeling aims to obtain transport properties at discrete concentration of ionic species with classical force fields via molecular dynamic simulations.

unit operations. In particular, we investigate small molecules analogues to the polyethylenimines often used in organic/inorganic mesoporous sorbents.

Carbon dioxide absorption onto a variety of sorbents including ionic liquids,[18−20] porous aromatic frameworks,[21] zeolites,[22,23] and aqueous amine solutions[24,25] has previously been investigated via computer simulations. The whole gamut of computer simulation techniques has been applied to the field, from ab initio investigations of the CO_2/sorbent interaction to the application of molecular dynamics (MD) and Monte Carlo (MC) simulation methods to obtain transport properties of the absorbed species and the absorption/adsorption capacity of the sorbent. For convenience, the sorbents mentioned above can be classified as physical, in which the interactions between CO_2 and the sorbent material is noncovalent, that is primarily based on van der Waals and Coulombic interactions, and chemical, in which a chemical reaction occurs with (essentially irreversible) covalent or ionic bond formation such as in the amine/CO_2 system. Most investigations using MD and MC simulations probe sorbents involving physical interactions with the CO_2 molecule because of challenges in simulating reactive systems with these techniques. It is possible, however, to tune the interaction between CO_2 and the sorbent to imitate the covalent bonding found in chemical systems by using data from ab initio calculations.[23] A second approach is to use ionic speciation,[24,26] which involves enumerating the most important molecular species in the system, including neutral molecules, anions, cations, and zwitterions, and preparing mixtures with discrete concentrations of a subset of the possible species to be simulated via MC and MD. A third approach involves parametrization of a reactive force field in which bonds between the atoms in the simulation are formed on the fly.[27] These force fields are invaluable tools in the simulation of reactive systems, but they are also computationally expensive and require substantial effort to parametrize. One such parametrization of the CO_2/amine reaction has been recently used to study the structural properties of CO_2/ionic liquid mixtures containing amine groups (for 1 ns simulations); however, the transport properties of such mixtures were not investigated.[28] We here select the ionic speciation approach since its moderate computational demands allow simulating long enough trajectories to obtain transport coefficients such as diffusivities.

The general methodology of this work (Figure 1) is to apply molecular dynamics (MD) simulations to determine physical and transport properties of mixtures of hexamethylenediamine (D6) or diethylenetriamine (DT) with CO_2. Our preliminary work (see Supporting Information) indicated that using a model where CO_2 is merely physisorbed in the amines fails to capture the extent of absorption and the trend in viscosity change that are observed experimentally. We show that accounting for the presence of ionic species is required to capture qualitatively the observed physical behavior of the reactive mixture. To include these effects we investigate two ionic speciation[24,26] models, one including anion and cation species, and a second including zwitterion species. Finally, we demonstrate that the transport properties obtained from MD simulations of the ionic speciated mixtures can be incorporated into a macroscopic model and, with sensible choices for other physical parameters, describe thermogravimetric data qualitatively.

MATERIALS, MODELS, AND METHODS

Ionic Speciation. The bulk of this investigation involves probing the transport properties of two component mixtures of D6 or DT with CO_2. The choice of these relatively small polyamine molecules is partially motivated by computational tractability. The rationale for choosing DT is that it is used for the extraction of acid gas and is representative of a class of larger polyethylenimine analogs that have been used in organic/inorganic composite materials for carbon capture applications.[11] D6 is an industrially relevant amine whose chemical structure provides an interesting contrast to DT since it lacks a secondary amine. We utilize ionic speciation to account approximately for the ionic species present in real mixtures.[24,26,29] The technique consists of building models of those ionic species most likely to be present in real mixtures and simulating systems with variable ratios of ionic to neutral species. Ionic speciation has been used previously to investigate the transport properties of amine containing ionic liquids upon absorption of CO_2[26] and of aqueous solutions of *N*-methyldiethanolamine and piperazine.[24] In addition, a similar technique has been used to investigate morphological and structural

DOI: 10.1021/acsami.5b04153
ACS Appl. Mater. Interfaces 2015, 7, 17603−17613

properties of lithium-neutralized ionomers as a function of neutralization level and ionic-content.[30]

Two representative ionic speciation models were used where only the primary amines form ionic groups: a single ion or anion model and a zwitterion model (cf., Figure 1). In the single ion model, each amine molecule may contain a single ionic group, making it an ammonium or a carbamate ion. There is a 1-to-1 ratio of anion-to-cation molecules in the single ion model to preserve the overall charge neutrality in the system. In the zwitterion model, all ionic molecules contain both the anion and cation groups, making them zwitterionic species. Both models are intended to be idealized realizations of the compositions of real mixtures, where many different ionic species are typically present.[31] Note that in our models the secondary amine in DT is never replaced with an ionic group, a simplification adopted to keep the number of compositions to simulate to a manageable but representative set, and justified by NMR data suggesting that the primary amines in DT are the most reactive (at least in aqueous solution).[31] Table 1 summarizes the chemical composition of every system simulated for this study.

Table 1. Molecular Compositions of Systems Investigated

		molecular species[a]			
speciation model	% negative groups	neut.	+	−	±
	diethylenetriamine (DT)				
neutral	0	250	0	0	0
zwitterion	10	225	0	0	25
	20	200	0	0	50
	30	175	0	0	75
	40	150	0	0	100
	50	125	0	0	125
single ion	10	200	25	25	0
	17	163	43	43	0
	33	83	83	83	0
	40	50	100	100	0
	50	0	125	125	0
	hexamethylenediamine (D6)				
neutral	0	208	0	0	0
zwitterion	10	180	0	0	20
	20	160	0	0	40
	30	140	0	0	60
	40	120	0	0	80
	50	100	0	0	100
single ion	10	160	20	20	0
	20	120	40	40	0
	30	80	60	60	0
	40	40	80	80	0
	50	0	100	100	0

[a]All systems include 2 free CO_2 molecules.

Force Field Development. To simulate D6 and DT, we adapt the TraPPE-EH[32] amine force field developed by Wick et al.[33] This force field has also been parametrized to model CO_2.[34] The TraPPE-EH force field is designed to be transferable, utilizing the minimum number of parameters to reproduce the equilibrium phase behavior of the modeled molecules. Because of its parametrization against experimental data at various temperatures, TraPPE-EH will be valid at the experimental temperature for CO_2 capture. Although the model is straightforward to implement, its adaptation to polyfunctional amines with nitrogen atoms separated by two carbon atoms such as DT was challenging. In the original TraPPE-EH force field, intramolecular nonbonded forces are calculated for united atoms, heavy atoms (C and N), and polar hydrogen separated by four or more bonds. Although this nonbonded exclusion rule is enough for monofunctional amines, it is problematic for multifunctional ones in which two nitrogen atoms are separated by three bonds as in DT. With the original rules, the interaction between such nitrogen atoms is excluded, leaving the charges located at the bound polar hydrogen unprotected. This approach results in an unstable model where the negative partial charges in the polar hydrogen attract strongly the positive charges in the nitrogen atom resulting in atom fusion. A similar problem was observed by the developers of TraPPE-EH when they attempted to model glycols.[35] To address this issue, we adopt the force field's rule originally meant for aliphatic hydrogen: the polar hydrogen atoms only interact intramolecularly when the nitrogen atoms they are bound to interact as well.

A torsional potential for the dihedral involving N−C−C−N atoms was parametrized since it was not available in the original force field. One such potential has been previously developed[36] but it deviates slightly from the one obtained here since different rules for the exclusion of intramolecular nonbonded interactions were used. In this work, we use ethylenediamine (EDA) as a small model from which we can obtain the energy of the N−C−C−N torsion as a function of the angle by means of ab initio calculations[37] at the MP2/6-31G* level. A minimum energy structure for EDA computed at a lower level of theory was obtained from the literature[38] and used as a starting point in our computations. The relaxed potential energy surface along the dihedral angle was obtained and compared to the one obtained with the TraPPE-EH force field. The energy of the torsional potential thus obtained was used to parametrize the dihedral functional form[33] (see Supporting Information).

Finally, we developed force field parameters to describe the ionic species present in our models. The TraPPE-EH model is typically parametrized against experimental vapor/liquid phase behavior data but this is not available for the ionic species. Here we hence follow the approach used by Maginn et al.[26] in which the CHELPg[39] method is used to obtain the partial charges for the ionic groups. Parameters for the nonbonded VDW interactions were obtained from the TraPPE-EH model for neutral molecules. The charges obtained by CHELPg were tuned to make them consistent with the TraPPE-EH approach. This tuning included making all aliphatic, nonalpha hydrogen/carbons neutral and making the net charge of the ammonium and carbamate ionic groups (including the α-carbon) sum to either −1 or 1, respectively. Finally, intramolecular angular and dihedral potentials for ionic groups were obtained from Maginn et al.,[26] while the bond lengths were kept fixed at their equilibrium positions via the SHAKE algorithm. The final force field parameters are listed in the Supporting Information as a DL_POLY field file.

Molecular Dynamics Simulation Method. MD simulations were performed with the dl_classic package.[40] Initial configurations at varying concentrations of neutral and ionic species were created by means of a Monte Carlo routine included in the Project Aten program.[41] Most simulations in our study contained two tracer CO_2 molecules that served to calculate the diffusivity of unreacted CO_2 in the system. We assume that such a small concentration of CO_2 has a negligible effect on the overall properties of the mixture. Partial overlaps in the initial configurations were removed by running short MD simulations (10^5 steps) with very small time steps (10^{-7} ps), force capping, and velocity rescaling. The systems were then equilibrated in the NPT ensemble for 2 ns, followed by 10 ns production runs. The Nose-Hoover thermostat and barostat with 1.0 ps relaxation times were used. Finally, NVT simulations at the equilibrium densities were performed for at least 12 ns and up to 20 ns depending on the particular system. A spherical cutoff of 12.0 Å was used for the nonbonded interactions and the electrostatics were treated with the damped, force shifted Coulomb sum[42,43] method with a precision of 10^{-6}. A time step of 2 fs was utilized and the system configuration was written every 0.5 ps. The SHAKE algorithm with 10^{-8} convergence parameter was used to keep all bond-lengths at their equilibrium values. All simulations were performed at 1 atm.

Thermogravimetry. The objective of the thermogravimetric experiments was to measure the CO_2 absorption on films of amine samples for comparison to a macroscopic model of the absorption process. Specifically, we first reproduced the data previously obtained for DT[11] as validation and then generated anew a similar data set for D6. All chemicals were purchased from Aldrich and were used as

DOI: 10.1021/acsami.5b04153
ACS Appl. Mater. Interfaces 2015, 7, 17603−17613

received, and the experimental methodology implemented was in accord to ref 11. Briefly, CO_2 absorption measurements were performed on a TA Instruments Q500 thermogravimetric analyzer. Dry, pure CO_2 (99.99% v/v) at 1 atm was used for absorption, while high purity N_2 was utilized as a preparation gas and for CO_2 desorption. A typical experiment consisted of placing 20 μL of amine in an aluminum sample pan. The sample was heated to 105 °C in a stream of N_2 for 2−5 min depending on the volatility of the material. The temperature was then decreased to the absorption temperature (typically 75 °C) at a rate of 20 °C min^{-1}. The sample was then exposed to CO_2 for 60 min in which the weight change of the sample was monitored. No correction due to the evaporation of the amine during the absorption period was applied as it was assumed that evaporation rate was negligible due to the solid film that forms upon CO_2 exposure.

RESULTS AND DISCUSSION

The density of a representative set of pure amines was computed by means of NPT ensemble MD simulations. Table 2 shows the density of selected amines using our adapted TraPPE-EH compared to experimental values at T = 298.15 K. Our simulation results agree with experimental values to within 3% in all cases indicating that our nonbonded interactions are accurate and perform similarly to the original TraPPE-EH force field. In the case of D6, the density was obtained from simulations that included two tracer CO_2 molecules. We have found through simulations with DT that the results vary insignificantly for simulations with or without a small concentration of CO_2 tracers.

Table 2. Density of Propylamine (PA), D6, EDA, DT, and Tetraethylenepentamine (TP) Obtained with the Adapted TraPPE-EH Force Field Compared to Experimental Values at T = 298 K[a]

amine	ρ_{MD} (g/mL)	ρ_{exp} (g/mL)	% diff
PA	0.708(4)	0.712[44]	0.5
D6	0.8608(4)[b]	c	c
EDA	0.905(3)	0.897[45]	1.0
DT	0.977(7)	0.954[46]	2.7
TP	1.02(1)	0.998[46]	1.3

[a]The number in parentheses is the uncertainty in the last digit of the computed density. [b]Obtained with a system that included CO_2 tracer molecules. [c]Substance is solid at T = 298 K.

Similarly, we obtained the density of DT or D6 as a function of the amount of COO^- species, temperature, and speciation model (Figure 2). As expected, the density increases with decreasing temperature, the effect being stronger at small COO^- concentrations. Except for the D6 single ion model, the density increases monotonically with charged molecule concentration. For the D6 single ion model, the density decreases slightly when the anion concentration is increased from 40% to 50% (mol/mol). For both DT and D6, the zwitterion model predicts higher density than the single ion model at high COO^- concentration, possibly indicating a tighter molecular packing of the zwitterions. Since the mass of our system increases with increasing concentration of the charged species, we compute the volume per amine molecule (not including CO_2, Figure 3) to check whether the changes in density are due to the increase in mass or due to variations in the volume of the system. For all cases except DT at 298 K, a minimum in the molecular volume is observed. These minima are not pronounced for the single ion model but are clearly visible for the zwitterion data sets. At T = 348 K, a temperature relevant to CO_2 capture experiments, the volume changes little as a function of CO_2 concentration, an observation that has implications for the macroscopic modeling of the absorption process (described later on). We also observe that for the D6 single ion model, the molecular volume increases sharply when the COO^- concentration increases from 40% to 50% (mol/mol), consistent with the sudden decrease in density observed for these systems in Figure 2. This system is the only D6 sample without any neutral molecules, which leads to a

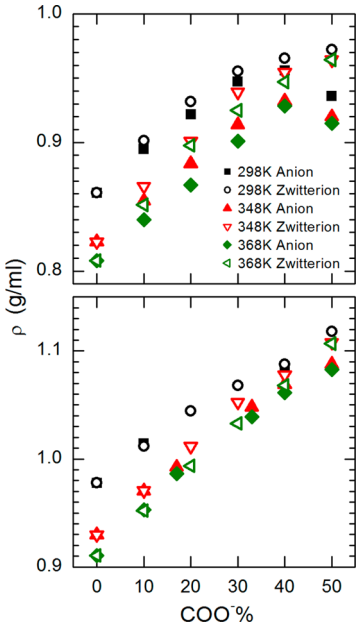

Figure 2. Density of D6 (top) and DT (bottom) as a function of the mole % of COO^- species, temperature, and speciation model. The estimated error bars (not shown) are smaller than the size of the symbols.

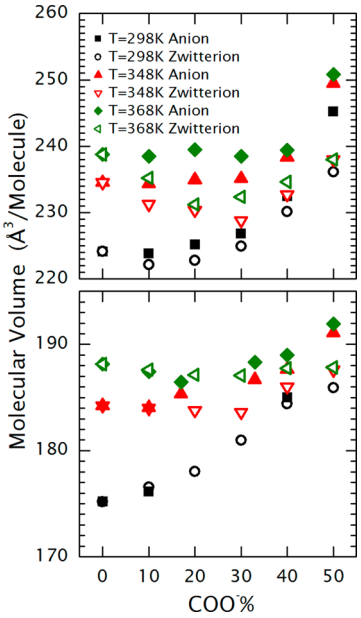

Figure 3. Volume per molecule of amine of D6 (top) and DT (bottom) as a function of the fraction of COO^- species, temperature, and speciation model.

DOI: 10.1021/acsami.5b04153
ACS Appl. Mater. Interfaces 2015, 7, 17603−17613

"glassier" relaxation of the structure (possibly hindering equilibration, see further discussion in next paragraphs).

To understand how the molecular mobility in the amine/CO_2 mixtures varies with the concentration of charged species, we compute the mean squared displacement (MSD) of the various molecular species in the simulation. Our primary objective is to get a sense of how the diffusion coefficient of CO_2 is affected by its concentration in the mixtures. In what follows, when we refer to physical "cross-links" we mean the localization in space of intermolecular ionic groups that interact strongly because of their electrostatic partial charges.

There are two CO_2 entities in the simulated mixture: (1) unreacted (physisorbed) CO_2 and (2) reacted (chemisorbed) CO_2 in an anionic form. We expect the diffusion of reacted CO_2 to be slower since it is bound to a larger, slower, and strongly interacting amine molecule. To confirm this hypothesis, we compute the MSD of free and bound CO_2 in the DT system at T = 348 K as a function of COO^- concentration (Figure 4). The slope of the upper dotted line

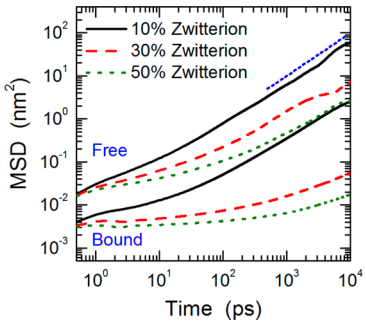

Figure 4. Mean squared displacement (MSD) of free and bound CO_2 for three zwitterion concentrations with DT. The short-dotted line atop represents a linear relationship between MSD and time.

in Figure 4 represents a linear relationship between MSD and time; it is plotted as a guide to detect when a simulated MSD curve has a comparable slope and hence has reached a diffusive regime. Error bars for the MSD curves (not shown for clarity) were obtained by the standard block-averaging method and used in the computation of the diffusion coefficients from the MSD curves (see Figure 5); note that these error values neglect the possible contributions from incomplete structural relaxation. The MSD of the reacted species is lower by at least 1 order of magnitude than that of the unreacted CO_2, a disparity that grows with increasing concentration of the charged groups. For the unreacted CO_2, the MSD reaches the linear regime allowing us to compute the diffusion coefficients. However, in most cases and especially at high ionic concentrations, the simulations were not long enough to sample diffusive behavior of the chemisorbed CO_2. For this reason, only diffusion coefficients of unreacted (tracer) CO_2 will be reported. The existence of two disparate time scales in the dynamic regimes for reacted and unreacted CO_2 molecules has implications for the macroscopic model we develop at the end of this section.

The diffusion coefficient of the free CO_2 species was calculated as a function of CO_2 concentration and temperature for DT (Figure 5a) and D6 (Figure 5b). The lines shown in Figures 5a and 5b represent a nonlinear fit of the data to an exponential function of the form

$$D^{P}_{CO_2} = D_0 e^{-[COO^-]/C} + D_{min} \quad (1)$$

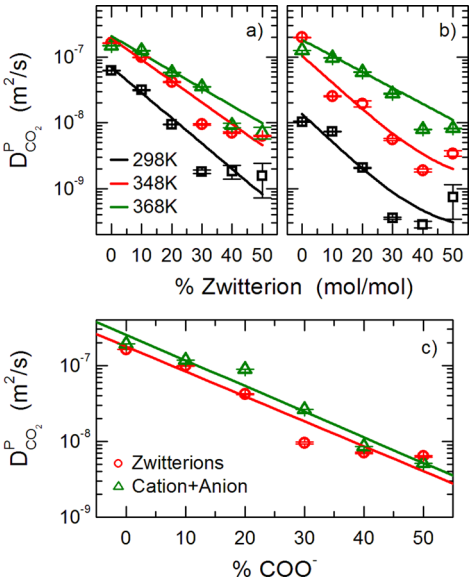

Figure 5. Diffusion coefficients obtained from the zwitterion model for (a) D6 and (b) DT as a function of concentration of the zwitterions for temperature equal to 298 (squares), 348 (circles), and 368 K (triangles). (c) A comparison of the zwitterion (circles) and single ion (triangles) models for D6 at T = 348 K. The lines represent nonlinear fits to the exponential relationship eq 1.

where D_0, C, and D_{min} are fitting parameters. The diffusion coefficient increases by at least 1 order of magnitude when increasing the temperature by 70 K. The diffusion coefficient also decreases as the amount of absorbed CO_2 increases, consistent with indirect experimental observations (see thermogravimetric data below). The data in Figure 5 and the correlations derived from them are the main result from the MD simulations. These correlations are incorporated into a macroscopic model to predict the absorption isotherms obtained from gravimetric experiments. Figure 5c shows a direct comparison between diffusion measurements of the zwitterion and single ion models. No significant differences exist between the two cases considered.

To illustrate the mobility trends for the reacted CO_2 molecules, we plot the MSD of the reacted carbon atoms as a function of temperature, reacted CO_2 concentration, and speciation model (Figure 6). As in Figure 4, the dotted blue line represents a linear relationship between MSD and time. The trends are the same as for free CO_2 tracer molecules. As the temperature decreases and the concentration of reacted CO_2 increases, the MSD of the carbamate functional group decreases as well. Note that only for the smallest concentrations of carbamate groups the MSD approaches the diffusive regime (parallel to dotted blue line), precluding us from developing correlations between the diffusion coefficient of the reacted species and its concentration. These observations give credence to our simplification that, relative to physisorbed CO_2 and to a first approximation, the diffusivity of reacted CO_2 may be neglected in the reaction-diffusion model described later.

An observation from thermogravimetric absorption experiments is that, after exposure to CO_2, the amine temporarily becomes highly viscous. In cases with long CO_2 absorption times, a solid-like layer forms at the amine-droplet/CO_2 interphase. We show that our simulated model exhibits the same behavior by monitoring the pressure autocorrelation function (PACF). The integral of the PACF can be related to

DOI: 10.1021/acsami.5b04153
ACS Appl. Mater. Interfaces 2015, 7, 17603−17613

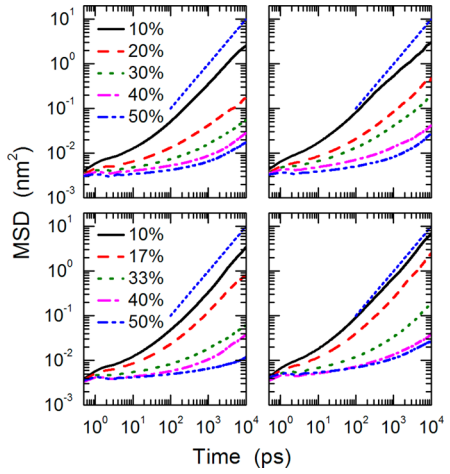

Figure 6. Mean squared displacement (MSD) as a function of simulation time for DT at 348 K (left), and 368 K (right) for the zwitterion model (top) and the single ion model (bottom). The concentration of the ionic species is shown in the legend. The straight dotted blue line represents a linear relationship between MSD and time, indicative of the diffusive regime.

the viscosity of a fluid via a Green–Kubo relationship.[47] Given the experimental observations, we expect that with increasing concentrations of ionic species, the integral of the PACF should exhibit a corresponding increase. This is exactly what we observe in Figure 7, where the integral of the PACF is plotted

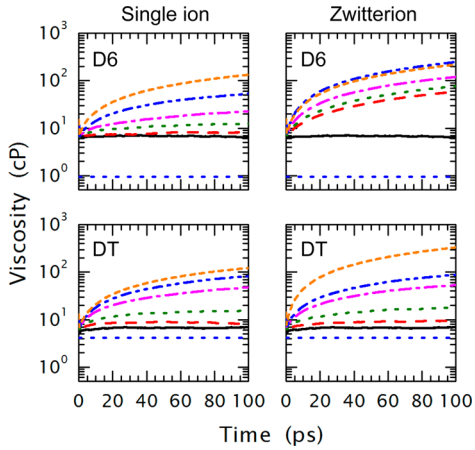

Figure 7. Integral of the PACF as a function of simulation time for the single ion (left) and zwitterion (right) models. For D6 (top) the concentration of ionic species are 0% (black), 10% (red), 20% (green), 30% (magenta), 40% (blue), and 50% (orange). For DT (bottom), the concentration of ionic species are 0% (black), 10% (red), 17% (green), 33% (magenta), 40% (blue), and 50% (orange). The blue short-dashed lines represent experimental viscosities at 298 and 353 K for DT and D6, respectively.

as a function of time and COO^- concentration. Note that since at higher concentrations of ionic species the integral of the autocorrelation function does not fully converge, we do not report single values for the viscosity of the simulated systems. The dashed blue lines in Figure 7 represent experimental values for the viscosity of the pure amines (see the figure caption). For D6 (top), the integral of the PACF for the single ion model (left) increases gradually with increasing ionic concentration. The total increase in the scale shown is of at least 2 orders of magnitude, a significant increase in mixture viscosity. The zwitterion model (right) exhibits a similar trend except that the increase in viscosity is abrupt, with only 10% of the ionic species resulting in 2 orders of magnitude increase in the system viscosity. This may be due to the bifunctional nature of the zwitterionic species and the increased likelihood of creating bridges between ionic centers in the mixture (some examples of such bridges will be shown later). For DT, both zwitterion and single ion models predict smooth increases in viscosity with increasing COO^- concentration. A possible explanation for this prediction is the tendency of the anions in this molecule to interact intramolecularly with the secondary amine, reducing the ability of the molecule to act as a bridge between ionic centers. The effect of temperature on viscosity was of secondary importance compared to that of ionic concentration and although the viscosity decreases with increasing temperature, it is difficult to differentiate statistically between the 348 and 368 K cases.

Our MSD and PACF data corroborate experimental observations of slowed dynamics upon CO_2 absorption. We now use the simulation results to provide insight into structure–property relationships by looking at selected radial distribution functions (RDFs) and simulation snapshots. Our hypothesis is that, upon CO_2 chemisorption, anion and cation formation leads to segregated ionic complexes that act like temporary cross-linkers within the system. The RDF data provides some evidence for this hypothesis.

The RDF allows us to gauge how close, on average, different type of atoms in the reactive CO_2/amine mixture are located relative to each other. Our principal interest is the distance between the carbon dioxide oxygen atoms and the amine hydrogens. As described before, there are two types of carbon dioxide groups in the system, free and bound ones. Figure 8 shows representative partial RDFs between amine hydrogen atoms and carbon dioxide oxygen at 348 K and 40% COO^- concentration. Partial RDFs at different ionic concentrations exhibit nearly identical trends to those shown in Figure 8. All types of amine hydrogens in the simulation exhibit coordination with the anionic groups. Of these, the coordination between reacted CO_2 groups and amine groups (as measured by the area under the corresponding RDF first peak) increases in the order: primary < secondary < ammonium (amine). The coordination between anionic and cationic groups is very strong providing evidence to our conjecture that these ionic centers act as physical cross-links in the reactive mixtures. There is no similar coordination between neutral CO_2 and the amine groups, possibly because free CO_2 is hindered from approaching the cations by the stronger coordination between anionic CO_2 and amine groups. This may explain why we observe faster diffusivity for nonreacted CO_2 molecules than for the reacted ones (see Figure 4).

In addition to the RDFs, we have performed a limited hydrogen bond analysis for the various interactions in the system to quantify the percentage of possible hydrogen bonds formed and their lifetime. To this end, we follow the approach in Maginn et al.[29] for hydrogen bond identification. For an interaction to count as a hydrogen bond, two criteria must be met: First, the distance between donor (ammonium nitrogen) and acceptor (carbamate oxygen) must be less than 3.3 Å; second, the angle between donor, hydrogen, and acceptor must be greater than 145°. We focus on the carbamate/ammonium interaction since it is the most common one observed according to the RDFs. For the zwitterion D6 model at 348

DOI: 10.1021/acsami.5b04153
ACS Appl. Mater. Interfaces 2015, 7, 17603–17613

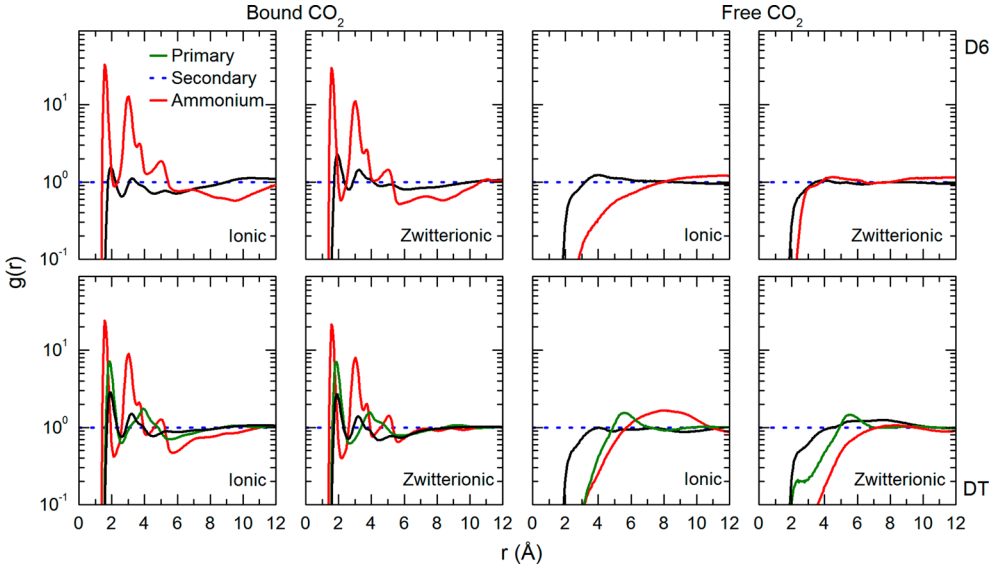

Figure 8. Partial radial distribution functions between amine and CO_2 groups at T = 348 K and ionic concentration of 40% as a function of amine, speciation model, and CO_2 species. The blue dotted line is to guide the eye and has a value of $g(r)$ = 1.

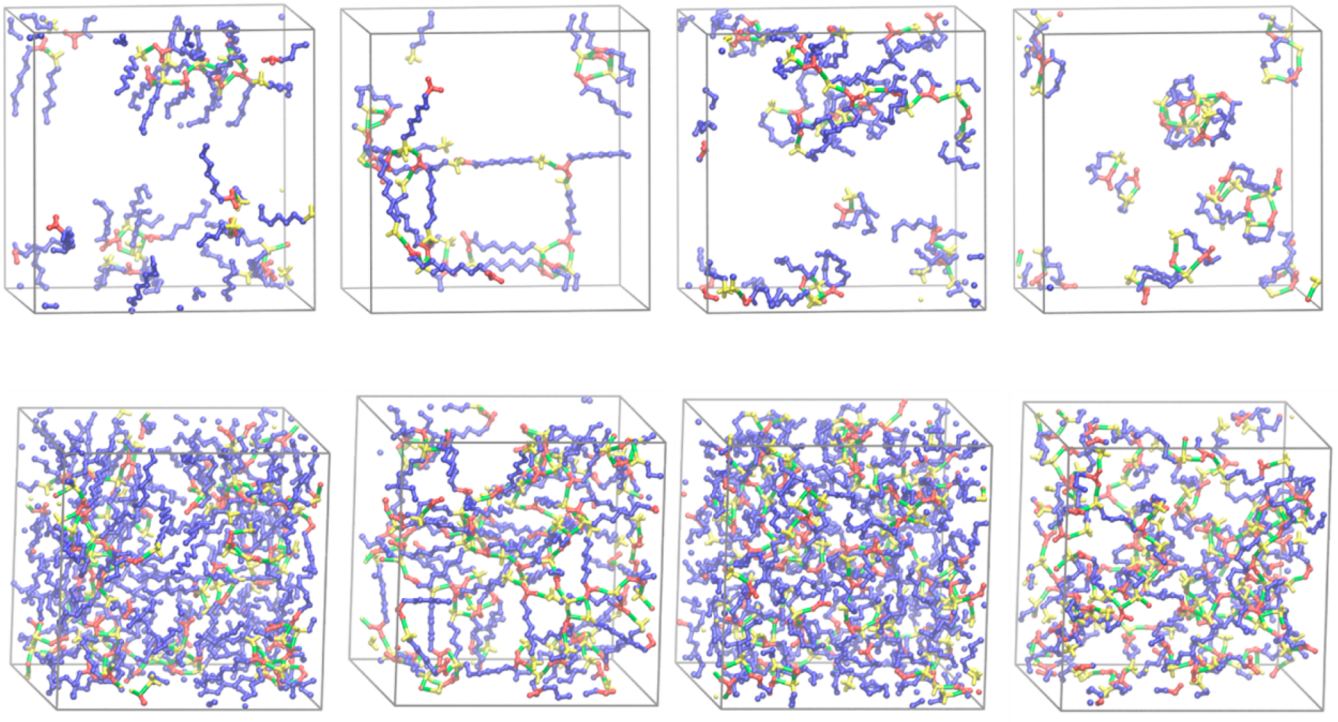

Figure 9. Snapshots of simulations for 10% (top) and 40% (bottom) COO^- concentration. From left to right: D6 single ion, D6 zwitterion, DT single ion, and DT zwitterion models. Blue represents nonionic parts of the molecule, red anionic, and yellow cationic. Green represents hydrogen bond interactions. Only charged molecules are shown and all side atoms are hidden for clarity.

K, an average of 2.2 hydrogen bonds per zwitterion are counted suggesting that some ammonium ions interact with more than two carbamate groups. We also observe an average distance between an ammonium hydrogen and a carbamate oxygen of 1.6 Å, in excellent agreement with the location of the first peak in the RDFs. Furthermore, the average lifetime of these hydrogen bond interactions were calculated to be at least 8.5 ps. For comparison, the average lifetime of hydrogen bonds in water is on the order of 0.25 ps.[48] The long average lifetimes of hydrogen bond interactions between ammonium and carbamate may explain the observed increase in viscosity and reduction in diffusivity as the amount of ionic groups in the reactive mixture increased.

To complement the information in the partial RDF plots, we provide select snapshots of our simulated systems to illustrate the cross-linking between ionic groups in Figure 9. The green "bonds" represent hydrogen bonding interactions between ammonium and carbamate groups; they have a maximum distance of 1.7 Å. The most interesting observations occur at the lowest concentration of ionic species (10%, top row). For

DOI: 10.1021/acsami.5b04153
ACS Appl. Mater. Interfaces 2015, 7, 17603−17613

the D6 system, we observe two morphologies depending on the speciation model. In the case of the single ion model, we observe reverse-micelle-like aggregates with ionic cores and protruding alkane tails. The range of molecules in each aggregate is from 2 to about 10 for this snapshot. For the D6-zwitterion model, we observe extended alkanes bridging ionic interaction sites. These bridges result in a single aggregate percolating the entire simulation box, which may explain the abrupt increase in viscosity for this system observed in Figure 7. The zwitterion-D6 system is the only one that exhibits a percolated network at such low concentrations of ionic species. For the DT single ion model, we observe a similar morphology to that of the D6 single ion model. However, for the DT zwitterion, we do not see the same percolation observed for the D6 case. We observe instead several small ionic cluster and even some self-interacting zwitterionic molecules. Increasing the concentration of ions in the system quickly increases the amount of "cross-linking" points as exhibited for all systems simulated at 40% COO^-. Under these conditions, the systems would have all become "gels".

The diffusion data obtained from MD simulations can be applied to macroscopic, continuum modeling by means of partial differential transport equations. We use such an approach to obtain data that can be qualitatively compared to thermogravimetric measurements on DT and D6. The typical thermogravimetric data set is shown in Figure 10 for both DT

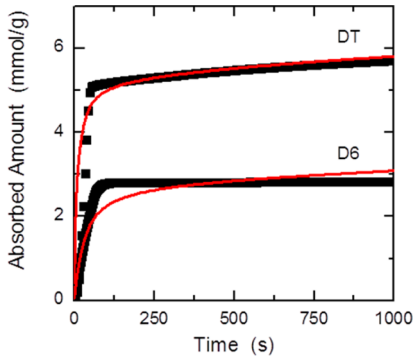

Figure 10. Absorption of CO_2 measured by TGA experiments (black squares) and predicted by our model (red lines) at T = 348 K.

and D6 at T = 348 K. The most important feature observed in this type of experiment is the appearance of two absorption rate regimes. When the amine is first exposed to CO_2, the sample weight increases rapidly indicating fast uptake of CO_2. Within a couple of minutes, the absorption rate decreases and a slow absorption regime ensues. In the case of D6, the slow absorption regime is essentially a plateau. A possible explanation for these observations is that the amine is reaching its saturation concentration of CO_2. This, however, is unlikely since the amount of CO_2 absorbed is much lower than that expected by the amount of amine groups available in the sample. An alternative explanation, and the one we favor, is that the initial absorption process slows the molecular transport of the surface layer of the amine, stalling further CO_2 absorption. This explanation is consistent with our MD results in that we observe a substantial decrease in the diffusion coefficient of CO_2 with increasing amount of chemisorbed CO_2 in the simulation.

We now proceed to describe the macroscopic model employed. Although the actual experimental system is inhomogeneous and entails a nonequilibrium process, we can use our MD results by assuming *local* equilibrium, that is, that simulations probed a nanodomain of a given chemical composition (and set physical properties). Accordingly, we make the diffusion coefficient of unreacted CO_2 to depend on the local chemical composition (chemisorbed CO_2) as obtained by MD simulation eq 1, hence allowing it to change in space and time. Given our MD results, we assume that the diffusion of reacted (chemisorbed) CO_2 molecules is very small compared to that of unreacted (physisorbed) CO_2 and that convection terms may be neglected. We also assume that diffusion occurs in a single dimension through the amine film (slab geometry) and that the thickness of the film is l = 1 mm. At the conditions of the absorption experiment, we assume that the reaction is irreversible and that, at the beginning of the absorption process, the process is reaction limited. As production of carbamate and ammonium ions increases with absorption time, the diffusion coefficient of unreacted CO_2 decreases, making the reaction diffusion limited. A simplified model of a thermogravimetric experiment is then described by the following equations:

$$\frac{\partial \Theta_C}{\partial \tau} = \frac{\partial}{\partial \zeta}\left(D(\Theta_-)\frac{\partial \Theta_C}{\partial \zeta}\right) - \mathrm{Dm}_A \Theta_C \Theta_A \quad (2)$$

$$\frac{\partial \Theta_-}{\partial \tau} = \mathrm{Dm}_C \Theta_C \Theta_A \quad (3)$$

$$\frac{\partial \Theta_+}{\partial \tau} = \mathrm{Dm}_C \Theta_C \Theta_A \quad (4)$$

$$\frac{\partial \Theta_A}{\partial \tau} = -\mathrm{Dm}_C \Theta_C \Theta_A \quad (5)$$

Where the concentration for the neutral (Θ_A) and the ionic species (Θ_+ and Θ_- for cationic and anionic concentrations, respectively) have been scaled by the initial amine concentration ($[A]_0$), the concentration for free CO_2 (Θ_C) is scaled by the free CO_2 concentration at the gas/liquid interface ($[CO_2]_0$), the nondimensional time is defined as $\tau = tD_0/l^2$, and the nondimensional length (ζ) has been scaled by the thickness of the film. Two dimensionless Damköhler-like parameters are defined as $\mathrm{Dm}_A = k_f[A]_0 l^2/D_0$ and $\mathrm{Dm}_C = k_f[CO_2]_0 l^2/D_0$. Here k_f represents the rate of the forward reaction, D_0 is defined as in eq 1, and $D(\Theta_-)$ is the concentration dependent diffusion defined in eq 1. Initial and boundary conditions for this system of equations are

$$\Theta_C = \Theta_+ = \Theta_- = 0 \ @ \ \tau = 0$$

$$\Theta_A = 1 \ @ \ \tau = 0$$

$$\frac{\partial \Theta_C}{\partial \zeta} = 0 \ @ \ \zeta = 0$$

$$\Theta_C = 1 \ @ \ \zeta = 1$$

In addition, no-flux boundary conditions for the neutral amine and ionic species are enacted at the boundaries of the liquid film. The model thus described contains two parameters that we treat as adjustable: Dm_A and $[CO_2]_0$. The reason for this is that experimental data is scarce for the rate of reaction between CO_2 and pure amines (nonaqueous systems) and the interfacial solubility of CO_2 in the amine is unknown. Note that we assume that the free CO_2 solubility is independent of the

DOI: 10.1021/acsami.5b04153
ACS Appl. Mater. Interfaces 2015, 7, 17603−17613

composition of the liquid, a likely oversimplification. This system of equations was solved using the finite element solver FiPy.[49]

Figure 10 shows the amount of absorbed CO_2 predicted by our model compared to experimental TGA data for D6 and DT using values obtained from the zwitterion model. The red lines were obtained by manually adjusting Dm_A and $[CO_2]_0$ until a good fit was obtained. The two adjustable parameters provide latitude in getting the model to agree with experimental results. For instance, the curves in Figure 10 correspond to values of $[CO_2]_0$ of 3 and 0.25 M and of Dm_A of 0.6 and 2 for DT and D6, respectively. (These values of $[CO_2]_0$ are of the same order of magnitude as the maximal concentration of chemisorbed CO_2 in the amines). Using the fitting parameter values yields a k_f in the order 1 M^{-1} min^{-1}, which is consistent with a fast reaction, although (as expected) it is significantly slower than the rates of reactions reported in aqueous solution.[4] The continuum model shows that the fast uptake and subsequent plateauing of the absorption curve observed in the experiments is consistent with an abrupt reduction of CO_2 diffusivity with concentration of chemisorbed CO_2 as given by the simulations. This does not show a unique cause-and-effect, but it provides a plausible microscopic mechanism for the macroscopic behavior. On the other hand, our model cannot replicate some characteristics of the absorption curves. First, the final slope of the absorption curve for D6 is noticeably different from that of the experimental system and could not be much improved by varying the adjustable parameters. Second, the transition from a fast absorption rate to a slower one is more abrupt in the experimental system for both DT and D6. In both cases, our model exhibits a more gradual change in the absorption rate. Given the major simplifications of our model, like the simplified speciation models adopted, these inconsistencies are not surprising and reveal some of the limitations of our approach. It could also be that in reality the concentration of ionic species is not as important as the instant in which a percolating network between the molecules is formed. More generally, a more abrupt dependence of the diffusion coefficient on the concentration of ionic species appears to be necessary to more closely capture the experimental trends (i.e., the exponential decay of the diffusion coefficient in eq 1 may not be suitable to quantitatively extrapolate the diffusivity at higher ionic concentrations, particularly in the case of D6). Indeed, compared to experimental absorption curves the MD simulation would seem to overpredict the values of $D(\Theta_-)$ at high anion concentrations. A summary of the parameters used for the model and a basic analysis of the sensitivity of the model to variations in such parameters is available in the Supporting Information.

Despite its limitations, the continuum model can be used to provide semiquantitative guidelines for the design of CO_2 absorption systems using pure polyamines likes those used in this work. Given the sharp drop in CO_2 diffusivity as the concentration of reacted CO_2 increases, only a thin layer of amine is really active (used) for a fixed contact time. For instance, for a 17 min contact time with DT, our model (Figure 10) predicts that a 1 mm-thick film will absorb ~6 mmol of CO_2 per gram of amine (absorption efficiency of 41%), while a 1 μm-thick film will achieve 13 mmol/g (absorption efficiency of 89%). Clearly, experimental platforms that can form very thin amine layers spread out over high-surface area supports (like mesoporous silica) via impregnation[13] or by covalent grafting[50] will be highly advantageous.

Concluding Remarks. Molecular dynamics simulations of mixtures of CO_2 with D6 or DT have been performed using an ionic speciation model. The diffusion coefficient, viscosity, and structural properties of the mixtures were measured as a function of temperature and composition. The diffusion coefficients obtained from MD simulations were fitted to an exponential decay form to parametrize the dependence of the diffusion coefficient of free CO_2 with the concentration of reacted CO_2. This parametrization allows the construction of a model absorption experiment analogous to TGA experimental measurements. The model thus built has good order of magnitude agreement with experimental results, showing an initial rapid uptake of CO_2 followed by a slow plateauing.

The results from MD simulations are consistent with qualitative experimental observations that the viscosity of the amine/CO_2 mixtures increases with CO_2 exposure time. Furthermore, the simulated models reveal that the ionic groups present in the system segregate and interact strongly. In particular, ammonium and carbamate ions form strong bonds that may lead to cross-linking points along the mixture. At high enough reacted CO_2 concentration, the system forms a percolated network of neutral chains united by ionic cores (which would manifest macroscopically by the gelling of the sample, as observed experimentally).

This work can be seen as a first step toward the multiscale modeling of CO_2 absorption in water-free polyamines that are either supported in organic/inorganic composite mesoporous materials or sprayed into a fine mist. Future work should be devoted to collect further experimental data to validate and calibrate such models, for example, to characterize the ionic species formed in the samples and the viscosity changes upon CO_2 chemisorption. Regarding the molecular modeling, the use of reactive force fields[27] should be considered to potentially capture the kinetics of ionic speciation and gelation, allowing for multicomponent mixtures of ionic species to develop. The effect of humidity in the CO_2 stream would also be important to model as the presence of water in the amine is expected to alter the way CO_2 becomes chemisorbed. Given the observed coupling between absorbent gelling behavior and low CO_2 diffusivity, molecular simulations can explore alternative polyamines that may form less viscous networks and hence allow faster absorption kinetics. Simulations of the amine-gas interface should also be conducted to elucidate the properties of the interfacial CO_2 absorbed layer, information that will be important to refine the relevant boundary condition used in the continuum model. Work along some of these lines is currently under way.

■ ASSOCIATED CONTENT

Supporting Information

The Supporting Information is available free of charge on the ACS Publications website at DOI: 10.1021/acsami.5b04153.

Physisorption model, the torsional potential for NCCN dihedrals, the results of the parametrization of the diffusion coefficient, and force field parameters (PDF)

■ AUTHOR INFORMATION

Corresponding Author

*E-mail: fe13@cornell.edu.

Present Address

§S.T.C.: Department of Chemical Engineering, Kettering University, Flint, Michigan 48504

DOI: 10.1021/acsami.5b04153
ACS Appl. Mater. Interfaces 2015, 7, 17603−17613

Notes

The authors declare no competing financial interest.

■ ACKNOWLEDGMENTS

This publication was based on work supported by Award No. KUS-C1-018-02, made by King Abdullah University of Science and Technology (KAUST). EPG gratefully acknowledges support from NPRP Grant # 5-1437-1−243 from the Qatar National Research Fund. The authors are also grateful to computer cycles supplied by the Extreme Science and Engineering Discovery Environment (XSEDE) which is supported by National Science Foundation grant number OCI-1053575.

■ REFERENCES

(1) U.S. EPA. Carbon Dioxide Emissions. http://www.epa.gov/climatechange/ghgemissions/gases/co2.html (accessed Oct 3, 2014).
(2) Rochelle, G. T. Amine Scrubbing for CO2 Capture. *Science* **2009**, *325*, 1652−1654.
(3) MacDowell, N.; Florin, N.; Buchard, A.; Hallett, J.; Galindo, A.; Jackson, G.; Adjiman, C. S.; Williams, C. K.; Shah, N.; Fennell, P. An Overview of CO2 Capture Technologies. *Energy Environ. Sci.* **2010**, *3*, 1645−1669.
(4) Dell'Amico, D. B.; Calderazzo, F.; Labella, L.; Marchetti, F.; Pampaloni, G. Converting Carbon Dioxide into Carbamato Derivatives. *Chem. Rev.* **2003**, *103*, 3857−3898.
(5) Tossell, J. A. What Happens at the Microscopic Level When CO2 Reacts with Ammonia or Amines in Solution or on Cryogenic Surfaces? *Energy Environ. Sci.* **2010**, *3*, 1079−1091.
(6) George, M.; Weiss, R. G. Chemically Reversible Organogels: Aliphatic Amines as "Latent" Gelators with Carbon Dioxide. *J. Am. Chem. Soc.* **2001**, *123*, 10393−10394.
(7) George, M.; Weiss, R. G. Chemically Reversible Organogels via "Latent" Gelators. Aliphatic Amines with Carbon Dioxide and Their Ammonium Carbamates. *Langmuir* **2002**, *18*, 7124−7135.
(8) Belmabkhout, Y.; Serna-Guerrero, R.; Sayari, A. Amine-Bearing Mesoporous Silica for CO_2 Removal from Dry and Humid Air. *Chem. Eng. Sci.* **2010**, *65*, 3695−3698.
(9) Serna-Guerrero, R.; Belmabkhout, Y.; Sayari, A. Modeling CO_2 Adsorption on Amine-Functionalized Mesoporous Silica: 1. A Semi-Empirical Equilibrium Model. *Chem. Eng. J.* **2010**, *161*, 173−181.
(10) Serna-Guerrero, R.; Sayari, A. Modeling Adsorption of CO_2 on Amine-Functionalized Mesoporous Silica. 2: Kinetics and Breakthrough Curves. *Chem. Eng. J.* **2010**, *161*, 182−190.
(11) Qi, G.; Wang, Y.; Estevez, L.; Duan, X.; Anako, N.; Park, A.-H. A.; Li, W.; Jones, C. W.; Giannelis, E. P. High Efficiency Nanocomposite Sorbents for CO2 Capture Based on Amine-Functionalized Mesoporous Capsules. *Energy Environ. Sci.* **2011**, *4*, 444−452.
(12) Qi, G.; Fu, L.; Duan, X.; Choi, B. H.; Abraham, M.; Giannelis, E. P. Mesoporous Amine-Bridged Polysilsesquioxane for CO2 Capture. *Greenhouse Gases: Sci. Technol.* **2011**, *1*, 1−7.
(13) Qi, G.; Fu, L.; Choi, B. H.; Giannelis, E. P. Efficient CO_2 Sorbents Based on Silica Foam with Ultra-Large Mesopores. *Energy Environ. Sci.* **2012**, *5*, 7368−7375.
(14) Labreche, Y.; Lively, R. P.; Rezaei, F.; Chen, G.; Jones, C. W.; Koros, W. J. Post-Spinning Infusion of Poly(ethyleneimine) into Polymer/silica Hollow Fiber Sorbents for Carbon Dioxide Capture. *Chem. Eng. J.* **2013**, *221*, 166−175.
(15) Monazam, E. R.; Shadle, L. J.; Miller, D. C.; Pennline, H. W.; Fauth, D. J.; Hoffman, J. S.; Gray, M. L. Equilibrium and Kinetics Analysis of Carbon Dioxide Capture Using Immobilized Amine on a Mesoporous Silica. *AIChE J.* **2013**, *59*, 923−935.
(16) Kalyanaraman, J.; Fan, Y.; Lively, R. P.; Koros, W. J.; Jones, C. W.; Realff, M. J.; Kawajiri, Y. Modeling and Experimental Validation of Carbon Dioxide Sorption on Hollow Fibers Loaded with Silica-Supported Poly(ethylenimine). *Chem. Eng. J.* **2015**, *259*, 737−751.
(17) Perry, R. J.; Wood, B. R.; Genovese, S.; O'Brien, M. J.; Westendorf, T.; Meketa, M. L.; Farnum, R.; McDermott, J.; Sultanova, I.; Perry, T. M.; Vipperla, R.; Wichmann, L. A.; Enick, R. M.; Hong, L.; Tapriyal, D. CO_2 Capture Using Phase-Changing Sorbents. *Energy Fuels* **2012**, *26*, 2528−2538.
(18) Aparicio, S.; Atilhan, M. Computational Study of Hexamethylguanidinium Lactate Ionic Liquid: A Candidate for Natural Gas Sweetening. *Energy Fuels* **2010**, *24*, 4989−5001.
(19) Cadena, C.; Anthony, J. L.; Shah, J. K.; Morrow, T. I.; Brennecke, J. F.; Maginn, E. J. Why Is CO2 so Soluble in Imidazolium-Based Ionic Liquids? *J. Am. Chem. Soc.* **2004**, *126*, 5300−5308.
(20) Perez-Blanco, M. E.; Maginn, E. J. Molecular Dynamics Simulations of CO2 at an Ionic Liquid Interface: Adsorption, Ordering, and Interfacial Crossing. *J. Phys. Chem. B* **2010**, *114*, 11827−11837.
(21) Babarao, R.; Dai, S.; Jiang, D. Functionalizing Porous Aromatic Frameworks with Polar Organic Groups for High-Capacity and Selective CO2 Separation: A Molecular Simulation Study. *Langmuir* **2011**, *27*, 3451−3460.
(22) Madison, L.; Heitzer, H.; Russell, C.; Kohen, D. Atomistic Simulations of CO_2 and N2 within Cage-Type Silica Zeolites. *Langmuir* **2011**, *27*, 1954−63.
(23) Vaidhyanathan, R.; Iremonger, S. S.; Shimizu, G. K. H.; Boyd, P. G.; Alavi, S.; Woo, T. K. Direct Observation and Quantification of CO_2 Binding within an Amine-Functionalized Nanoporous Solid. *Science* **2010**, *330*, 650−653.
(24) Farmahini, A. H.; Kvamme, B.; Kuznetsova, T. Molecular Dynamics Simulation Studies of Absorption in Piperazine Activated MDEA Solution. *Phys. Chem. Chem. Phys.* **2011**, *13*, 13070−13081.
(25) Maiti, A.; Bourcier, W. L.; Aines, R. D. Atomistic Modeling of CO_2 Capture in Primary and Tertiary Amines − Heat of Absorption and Density Changes. *Chem. Phys. Lett.* **2011**, *509*, 25−28.
(26) Gutowski, K. E.; Maginn, E. J. Amine-Functionalized Task-Specific Ionic Liquids: A Mechanistic Explanation for the Dramatic Increase in Viscosity upon Complexation with CO2 from Molecular Simulation. *J. Am. Chem. Soc.* **2008**, *130*, 14690−14704.
(27) Van Duin, A. C. T.; Dasgupta, S.; Lorant, F.; Goddard, W. A. ReaxFF: A Reactive Force Field for Hydrocarbons. *J. Phys. Chem. A* **2001**, *105*, 9396−9409.
(28) Zhang, B.; van Duin, A. C. T.; Johnson, J. K. Development of a ReaxFF Reactive Force Field for Tetrabutylphosphonium Glycinate/CO2Mixtures. *J. Phys. Chem. B* **2014**, *118*, 12008−12016.
(29) Wu, H.; Shah, J. K.; Tenney, C. M.; Rosch, T. W.; Maginn, E. J. Structure and Dynamics of Neat and CO 2 -Reacted Ionic Liquid Tetrabutylphosphonium 2-Cyanopyrrolide. *Ind. Eng. Chem. Res.* **2011**, *50*, 8983−8993.
(30) Bolintineanu, D. S.; Stevens, M. J.; Frischknecht, A. L. Atomistic Simulations Predict a Surprising Variety of Morphologies in Precise Ionomers. *ACS Macro Lett.* **2013**, *2*, 206−210.
(31) Hartono, A.; da Silva, E. F.; Grasdalen, H.; Svendsen, H. F. Qualitative Determination of Species in DETA−H_2O−CO_2 System Using ^{13}C NMR Spectra. *Ind. Eng. Chem. Res.* **2007**, *46*, 249−254.
(32) Chen, B.; Siepmann, J. I. Transferable Potentials for Phase Equilibria. 3. Explicit-Hydrogen Description of Normal Alkanes. *J. Phys. Chem. B* **1999**, *103*, 5370−5379.
(33) Wick, C. D.; Stubbs, J. M.; Rai, N.; Siepmann, J. I. Transferable Potentials for Phase Equilibria. 7. Primary, Secondary, and Tertiary Amines, Nitroalkanes and Nitrobenzene, Nitriles, Amides, Pyridine, and Pyrimidine. *J. Phys. Chem. B* **2005**, *109*, 18974−18982.
(34) Potoff, J. J.; Siepmann, J. I. Vapor−liquid Equilibria of Mixtures Containing Alkanes, Carbon Dioxide, and Nitrogen. *AIChE J.* **2001**, *47*, 1676−1682.
(35) Stubbs, J. M.; Potoff, J. J.; Siepmann, J. I. Transferable Potentials for Phase Equilibria. 6. United-Atom Description for Ethers, Glycols, Ketones, and Aldehydes. *J. Phys. Chem. B* **2004**, *108*, 17596−17605.
(36) Orozco, G. a; Nieto-Draghi, C.; Mackie, A. D.; Lachet, V. Transferable Force Field for Equilibrium and Transport Properties in Linear, Branched, and Bifunctional Amines I. Primary Amines. *J. Phys. Chem. B* **2011**, *115*, 14617−25.

DOI: 10.1021/acsami.5b04153
ACS Appl. Mater. Interfaces 2015, 7, 17603−17613

(37) Frisch, M. J.; Trucks, G. W.; Schlegel, H. B.; Scuseria, G. E.; Robb, M. A.; Cheeseman, J. R.; Scalmani, G.; Barone, V.; Mennucci, B.; Petersson, G. A.; Nakatsuji, H.; Caricato, M.; Li, X.; Hratchian, H. P.; Izmaylov, A. F.; Bloino, J.; Zheng, G.; Sonnenberg, J. L.; Hada, M.; Ehara, M.; Toyota, K.; Fukuda, R.; Hasegawa, J.; Ishida, M.; Nakajima, T.; Honda, Y.; Kitao, O.; Nakai, H.; Vreven, T.; Montgomery, J. A., Jr.; Peralta, J. E.; Ogliaro, F.; Bearpark, M.; Heyd, J. J.; Brothers, E.; Kudin, K. N.; Staroverov, V. N.; Kobayashi, R.; Normand, J.; Raghavachari, K.; Rendell, A.; Burant, J. C.; Iyengar, S. S.; Tomasi, J.; Cossi, M.; Rega, N.; Millam, J. M.; Klene, M.; Knox, J. E.; Cross, J. B.; Bakken, V.; Adamo, C.; Jaramillo, J.; Gomperts, R.; Stratmann, R. E.; Yazyev, O.; Austin, A. J.; Cammi, R.; Pomelli, C.; Ochterski, J. W.; Martin, R. L.; Morokuma, K.; Zakrzewski, V. G.; Voth, G. A.; Salvador, P.; Dannenberg, J. J.; Dapprich, S.; Daniels, A. D.; Farkas, O.; Foresman, J. B.; Ortiz, J. V.; Cioslowski, J.; Fox, D. J. *Gaussian 09*, revision A.1; Gaussian, Inc.: Wallingford, CT, 2009; http://www.gaussian.com/g_prod/g09.htm (accessed October 2013).

(38) Van Alsenoy, C.; Siam, K.; Ewbank, J. D.; Schäfer, L. Ab Initio Studies of Structural Features Not Easily Amenable to Experiment. *J. Mol. Struct.: THEOCHEM* **1986**, *136*, 77−91.

(39) Breneman, C. M.; Wiberg, K. B. Determining Atom-Centered Monopoles from Molecular Electrostatic Potentials. The Need for High Sampling Density in Formamide Conformational Analysis. *J. Comput. Chem.* **1990**, *11*, 361−373.

(40) Smith, W.; Forester, T. R.; Todorov, I. T. DL_POLY Classic [Computer Program], version 1.7. https://ccpforge.cse.rl.ac.uk/gf/project/dl_poly_classic/ (accessed May 2013).

(41) Youngs, T. G. A. Aten−an Application for the Creation, Editing, and Visualization of Coordinates for Glasses, Liquids, Crystals, and Molecules. *J. Comput. Chem.* **2010**, *31*, 639−648.

(42) Wolf, D.; Keblinski, P.; Phillpot, S. R.; Eggebrecht, J. Exact Method for the Simulation of Coulombic Systems by Spherically Truncated, Pairwise r^{-1} Summation. *J. Chem. Phys.* **1999**, *110*, 8254−8282.

(43) Fennell, C. J.; Gezelter, J. D. Is the Ewald Summation Still Necessary? Pairwise Alternatives to the Accepted Standard for Long-Range Electrostatics. *J. Chem. Phys.* **2006**, *124*, 234104.

(44) Kinart, C. M.; Kinart, W. J.; Chęcińska-Majak, D. Density, Relative Permittivity, and Viscosity at Various Temperatures for 2-Methoxyethanol + Propylamine Mixtures. *J. Chem. Eng. Data* **2002**, *47*, 1537−1539.

(45) Proutiere, A.; Megnassan, E.; Hucteau, H. Refractive Index and Density Variations in Pure Liquids: A New Theoretical Relation. *J. Phys. Chem.* **1992**, *96*, 3485−3489.

(46) Wypych, G. *Knovel Solvents—A Properties Database*; ChemTec Publishing: Toronto, Canada, 2003.

(47) McQuarrie, D. A. *Statistical Mechanics*, 1st ed.; Harper and Row: New York, 1976.

(48) Martiniano, H. F. M. C.; Galamba, N. Insights on Hydrogen-Bond Lifetimes in Liquid and Supercooled Water. *J. Phys. Chem. B* **2013**, *117*, 16188−16195.

(49) Guyer, J. E.; Wheeler, D.; Warren, J. A. FiPy: Partial Differential Equations with Python. *Comput. Sci. Eng.* **2009**, *11*, 6−15.

(50) Qi, G.; Fu, L.; Giannelis, E. P. Sponges with Covalently Tethered Amines for High-Efficiency Carbon Capture. *Nat. Commun.* **2014**, *5*, 5796.

DOI: 10.1021/acsami.5b04153
ACS Appl. Mater. Interfaces 2015, 7, 17603−17613